16th European Signal Processing Conference (EUSIPCO 2008), Lausanne, Switzerland, August 25-29, 2008, copyright by EURASIP

LOCALIZATION AND ESTIMATION OF MULTIPLE TARGETS FOR MIMO RADARS USING COVARIANCE MATCHING TECHNIQUES

Wei Xia and Zishu He

School of Electronic Engineering,
University of Electronic Science and Technology of China,
Chengdu, 610054, P.R. China,
email: wx@uestc.edu.cn, zshe@uestc.edu.cn

ABSTRACT

A multiple-input multiple output (MIMO) radar system uses multiple antennas to simultaneously transmit independent signals to illuminate targets, and multiple antennas to receive the reflected signals. The covariance structure of the received signals is analyzed, and the covariance matching estimation technique (COMET) is applied to solve the problem of multiple-target localization and estimation in MIMO radar systems. The performance of the proposed method is validated by numerical simulations.

1. INTRODUCTION

Motivated by the recently development of multiple-input multiple-output (MIMO) communication systems, the concept of MIMO radars is proposed by Fishler *et al.* [1]. The MIMO radar system has received increasing interest for its potential capability of insensitivity to the radar cross section (RCS) fluctuations [1, 2], high-resolution spatial spectral estimates [3–6], and flexible spatial transmit beam pattern design [7, 8].

Roughly speaking, the MIMO radar models may be categorized into two classes [6]. In one class, the transmit and receive antennas are closely spaced for coherent transmitting and receiving [4, 7]. In the other class, the transmit antennas are sparsely spaced to obtain spatial diversity. In this class, the antennas in the receiver array may be either sparsely placed to achieve receive spatial diversity [2], or closely spaced to implement coherent processing, e.g., direction finding [5].

In this proposal, we consider the recently proposed *statistical* MIMO radar model by Lehmann *et al.* [5], in which the transmit antennas are widely separated to exploit spatial diversity, while the receive antennas are closely spaced for direction finding. The propagating paths from the transmit array to the target and the scattering target are described by the stochastic fading vector. For the single target case, the delay-and-sum beamformer is optimal in the maximum likelihood (ML) sense, and has been applied to estimate the angle of a *single* target in [5]. The estimation of other parameters, e.g., the statistics of the fading vector and the noise parameters, is not further considered in [5]. We herein extend the model proposed in [5] to the more general multiple-target case, and apply the covariance matching estimation technique (COMET) [9] to obtain the angle estimates as well as other parameters of the MIMO radar system. We demonstrate through numerical simulations that the algorithm performs well in mild conditions.

The rest of this paper is organized as follows. In Section 2, the multiple-target statistical MIMO radar model is described. In Section 3, the covariance structure of the observed data vector is analyzed, and the covariance matching technique is applied to estimate the angles of multiple targets as well as other related parameters. In Section 4, simulation results are presented to illustrate the performance of the proposed method. The main results of this proposal are concluded in Section 5.

2. SIGNAL MODEL

Consider the discrete-time baseband MIMO radar model with K transmit antennas and M receive antennas

$$\mathbf{x}[n] = \mathbf{H}\mathbf{s}[n] + \mathbf{v}[n] \tag{1}$$

where $\mathbf{x}[n] \in \mathbb{C}^{M\times 1}$ is the noisy data vector, $\mathbf{s}[n] \in \mathbb{C}^{K\times 1}$ is the vector of complex envelope of the narrow-band signals illuminating the target, and $\mathbf{v}[n] \in \mathbb{C}^{M\times 1}$ is the additive Gaussian noise vector uncorrelated with the signal $\mathbf{s}[n]$.

The $M \times K$ channel matrix of the MIMO radar model is given by [5]

$$\mathbf{H} = \mathbf{a}(\theta)\boldsymbol{\alpha}^T \tag{2}$$

where the superscript $(\cdot)^T$ denotes matrix/vector transposition, $\boldsymbol{\alpha} \in \mathbb{C}^{K\times 1}$ is the target fading vector. The components $\alpha_k, k = 1, \cdots, K$ of the vector $\boldsymbol{\alpha}$ are zero-mean, unit-variance, independent, identical distributed (i.i.d.) circularly symmetric complex Gaussian random variables [1]. The RCS fluctuations (accordingly, $\boldsymbol{\alpha}$) are assumed herein to vary independently from pulse to pulse in one scan. This is the extension of the Swerling case-II. The receiver array is assumed to be a uniform linear array (ULA), and the steering vector of the receiver array is given by

$$\mathbf{a}(\theta) = \left[1, e^{-j2\pi \sin(\theta) d_r}, \cdots, e^{-j2\pi \sin(\theta)(M-1)d_r}\right]^T \tag{3}$$

where θ is the angle of the target with respect to the receiver array, and d_r is the inter-element distance of the receiver array in wavelengths.

When there exist L targets, the received signal at the nth snapshot is the superposition of all contributions due to mul-

This work was supported by the National Natural Science Foundation of China under Grant NO. 60672044.

[1] A circularly symmetric complex Gaussian random variable is a random variable $z = x + jy \sim CN(0, \sigma^2)$, where $x, y \sim N(0, \sigma^2/2)$ are i.i.d. Gaussian.

tiple targets and can be written as

$$\mathbf{x}[n] = \sum_{l=1}^{L} \mathbf{H}_l \mathbf{s}[n] + \mathbf{v}[n] = \sum_{l=1}^{L} \mathbf{a}(\theta_l)\boldsymbol{\alpha}_l^T \mathbf{s}[n] + \mathbf{v}[n], \quad n = 0, \cdots, N-1 \quad (4)$$

where $\boldsymbol{\alpha}_l$ and θ_l are the fading vector and angle of the lth target, respectively, and N is the total number of snapshots in one scan. By defining the direction matrix

$$\mathbf{A} \triangleq \mathbf{A}(\boldsymbol{\theta}) = [\mathbf{a}(\theta_1) \quad \mathbf{a}(\theta_2) \quad \cdots \quad \mathbf{a}(\theta_L)] \in \mathbb{C}^{M \times L} \quad (5)$$

and the fading matrix

$$\mathbf{B} = [\boldsymbol{\alpha}_1 \quad \boldsymbol{\alpha}_2 \quad \cdots \quad \boldsymbol{\alpha}_L]^T \in \mathbb{C}^{L \times K} \quad (6)$$

the signal model (4) can be also expressed as

$$\mathbf{x}[n] = \mathbf{A}\mathbf{B}\mathbf{s}[n] + \mathbf{v}[n], \qquad n = 0, \cdots, N-1. \quad (7)$$

where

$$\boldsymbol{\theta} = [\theta_1 \quad \theta_2 \quad \cdots \quad \theta_L]^T \quad (8)$$

It is assumed that the number of targets L is known *a priori*. Moreover, the number of targets is assumed to be less than the number of antennas of the receiver array, i.e., $L < M$. For the sake of brevity, it is assumed that the fading vectors of different targets are uncorrelated, i.e.,

$$\mathbb{E}\left\{\boldsymbol{\alpha}_l^H \boldsymbol{\alpha}_k\right\} = \begin{cases} \mathbb{E}\left\{\|\boldsymbol{\alpha}_l\|^2\right\}, & l = k \\ 0, & l \neq k \end{cases} \quad (9)$$

where $\mathbb{E}\{\cdot\}$, $(\cdot)^H$ and $\|\cdot\|$ denote mathematical expectation, matrix conjugate transposition, and Euclidean norm, respectively. The independence of the fading coefficients of different targets is further assumed, i.e.,

$$\mathbb{E}\left\{\alpha_{l,p}^* \alpha_{k,q}\right\} = 0, \qquad l \neq k \quad (10)$$

where $\alpha_{l,p}$ and $\alpha_{k,q}$ denote the pth and qth fading coefficients of the lth and kth targets, respectively, and the superscript $(\cdot)^*$ denotes the complex conjugate operator. Note that $\|\sqrt{2}\boldsymbol{\alpha}_l\|^2$ follows a χ^2_{2K} chi-square distribution with $2K$ degrees of freedom, and hence

$$\rho_l \triangleq \mathbb{E}\left\{\|\boldsymbol{\alpha}_l\|^2\right\} = K, \qquad l = 1, \cdots, L. \quad (11)$$

Note that (11) may not hold any more in the case of correlated target fading, i.e., the components of the fading vector $\boldsymbol{\alpha}_l$ of the lth target are correlated, $l = 1, \cdots, L$ [5]. Therefore, when there is unknown (correlated) fading, the estimate of the target fading statistics may be useful for target localization and classification.

The transmitted signals are assumed to be orthogonal and the covariance matrix of the transmitted signals is given by

$$\mathbb{E}\left\{\mathbf{s}[n]\mathbf{s}^H[n]\right\} = \sigma_s^2 \mathbf{I}_K \quad (12)$$

where σ_s^2 is the average power of the transmitted signals, and $\mathbf{I}_K$ is the identity matrix of size K. The noise vector $\mathbf{v}[n]$ is assumed to be temporally white with zero mean, the covariance matrix $\mathbf{Q}(\boldsymbol{\sigma}) = \mathbb{E}\left\{\mathbf{v}[n]\mathbf{v}^H[n]\right\}$, where $\boldsymbol{\sigma}$ is the unknown parameter vector. The noise $\mathbf{v}[n]$ is assumed to be uncorrelated with the probing signals $\mathbf{s}[n]$.

3. COVARIANCE MATCHING ESTIMATION

3.1 Covariance Matrix Analysis

As the noise $\{\mathbf{v}[n]\}$ is uncorrelated with the transmitted signals $\{\mathbf{s}[n]\}$, the covariance matrix of the received signals $\{\mathbf{x}[n]\}$ may be expressed as

$$\mathbf{R}(\boldsymbol{\theta}, \boldsymbol{\rho}, \boldsymbol{\sigma}) \triangleq \mathbb{E}\left\{\mathbf{x}[n]\mathbf{x}^H[n]\right\} = \mathbf{R}_s(\boldsymbol{\theta}, \boldsymbol{\rho}) + \mathbf{Q}(\boldsymbol{\sigma}) \quad (13)$$

where

$$\boldsymbol{\rho} \triangleq [\rho_1 \quad \cdots \quad \rho_L]^T \quad (14)$$

consists of the second order statistics of the fading of all L targets, and the columns of

$$\mathbf{R}_s(\boldsymbol{\theta}, \boldsymbol{\rho}) = \mathbb{E}\left\{\mathbf{A}\mathbf{B}\mathbf{s}[n]\mathbf{s}^H[n]\mathbf{B}^H\mathbf{A}^H\right\} \triangleq \mathbf{A}\mathbf{P}\mathbf{A}^H \quad (15)$$

span the signal subspace.

The (k, l)th entry of the *effective* source signal covariance matrix $\mathbf{P} = \mathbb{E}\left\{\mathbf{B}\mathbf{s}[n]\mathbf{s}^H[n]\mathbf{B}^H\right\}$ is given by

$$\mathbf{P}_{k,l} = \mathbb{E}\left\{\boldsymbol{\alpha}_k^T \mathbf{s}[n]\mathbf{s}^H[n]\boldsymbol{\alpha}_l^*\right\} \qquad k, l = 1, \cdots, L \quad (16)$$

where $(\cdot)^*$ denotes the complex conjugate. Using the trace identity $\mathrm{tr}\{\mathbf{XY}\} = \mathrm{tr}\{\mathbf{YX}\}$, (16) may be expressed as

$$\begin{aligned} \mathbf{P}_{k,l} &= \mathbb{E}\left\{\mathrm{tr}\left\{\boldsymbol{\alpha}_l^* \boldsymbol{\alpha}_k^T \mathbf{s}[n]\mathbf{s}^H[n]\right\}\right\} \\ &= \mathrm{tr}\left\{\mathbb{E}\left\{\boldsymbol{\alpha}_l^* \boldsymbol{\alpha}_k^T \mathbf{s}[n]\mathbf{s}^H[n]\right\}\right\}. \end{aligned} \quad (17)$$

Since both of the fading vectors $\boldsymbol{\alpha}_k$ and $\boldsymbol{\alpha}_l$ are uncorrelated with the transmitted signals $\mathbf{s}[n]$, we have

$$\begin{aligned} \mathbf{P}_{k,l} &= \mathrm{tr}\left\{\mathbb{E}\left\{\boldsymbol{\alpha}_l^* \boldsymbol{\alpha}_k^T\right\}\mathbb{E}\left\{\mathbf{s}[n]\mathbf{s}^H[n]\right\}\right\} \\ &= \sigma_s^2 \mathbb{E}\left\{\boldsymbol{\alpha}_l^H \boldsymbol{\alpha}_k\right\}. \end{aligned} \quad (18)$$

where we have used the assumption of the orthogonal transmitted signals (12). Hence, due to the independence assumption (9), theoretically, $\mathbf{P}$ is a diagonal matrix with identical entries on the main diagonal (cf. (11))

$$\mathbf{P} = \mathrm{diag}\{\rho_1, \cdots, \rho_L\}. \quad (19)$$

Note that the last equation results from the ideal assumption of (i) the orthogonal probing signals (12), and (ii) the independence of the fading vectors (9) and (10). In the cases that correlated transmitted signals are used, or the components of the fading vector $\boldsymbol{\alpha}_l$ of the lth target are correlated, $l = 1, \cdots, L$ [5], the main diagonal entries of $\mathbf{P}$ may deviate from the ideal values. Further, in practical engineering, if only finite samples are available, the statistical independence of the fading coefficients may be not satisfied strictly, and hence the deviation of the matrix $\mathbf{P}$ occurs as well. The interested readers are referred to [10] for further discussion on this issue. For the sake of simplicity, we consider the ideal case of (19) without loss of generality. The method described herein can be applied in a straightforward manner for the more practical values of $\mathbf{P}$.

Now consider vectorizing the covariance matrix $\mathbf{R}(\boldsymbol{\theta}, \boldsymbol{\rho}, \boldsymbol{\sigma})$ (i.e., stacking the columns of a matrix on top of one other)

$$\begin{aligned} \mathbf{r}(\boldsymbol{\theta}, \boldsymbol{\rho}, \boldsymbol{\sigma}) &\triangleq \mathrm{vec}(\mathbf{R}(\boldsymbol{\theta}, \boldsymbol{\rho}, \boldsymbol{\sigma})) \\ &= \mathrm{vec}(\mathbf{R}_s(\boldsymbol{\theta}, \boldsymbol{\rho})) + \mathrm{vec}(\mathbf{Q}(\boldsymbol{\sigma})). \end{aligned} \quad (20)$$

By using the identity

$$\mathrm{vec}(\mathbf{XYZ}) = (\mathbf{Z}^T \otimes \mathbf{X})\,\mathrm{vec}(\mathbf{Y}), \tag{21}$$

we obtain

$$\begin{aligned}\mathrm{vec}(\mathbf{R}_s(\boldsymbol{\theta},\boldsymbol{\rho})) &= (\mathbf{A}^* \otimes \mathbf{A})\,\mathrm{vec}(\mathbf{P}) \\ &= (\mathbf{A}^* \otimes \mathbf{A})\,\boldsymbol{\Gamma}\boldsymbol{\rho}\end{aligned} \tag{22}$$

where $\otimes$ denotes the Kronecker product, and $\boldsymbol{\Gamma}$ is a constant matrix dependent on the dimension of $\mathbf{P}$. For example, if $\mathbf{P} = \mathrm{diag}\{\rho_1, \rho_2\}$, then the transpose of $\boldsymbol{\Gamma}$ is given by

$$\boldsymbol{\Gamma}^T = \begin{bmatrix} 1 & 0 & 0 & 0 \\ 0 & 0 & 0 & 1 \end{bmatrix}.$$

Similar to the treatment of [9], we consider herein a structured noise covariance model $\mathbf{Q} = \sum_{i=0}^{M} \sigma_i \mathbf{Q}_i$. Thus, we have

$$\mathrm{vec}(\mathbf{Q}) = \sum_{i=0}^{M} \sigma_i\,\mathrm{vec}(\mathbf{Q}_i) = \boldsymbol{\Sigma}\boldsymbol{\sigma} \tag{23}$$

with

$$\begin{aligned}\boldsymbol{\Sigma} &\triangleq [\mathrm{vec}(\mathbf{Q}_1) \quad \cdots \quad \mathrm{vec}(\mathbf{Q}_M)] \in \mathbb{C}^{M^2 \times M}, \\ \boldsymbol{\sigma} &\triangleq [\sigma_1 \quad \cdots \quad \sigma_M]^T \in \mathbb{C}^{M \times 1}.\end{aligned} \tag{24}$$

Insertion of (22) and (23) into (20) yields

$$\begin{aligned}\mathbf{r}(\boldsymbol{\theta},\boldsymbol{\rho},\boldsymbol{\sigma}) &= (\mathbf{A}^* \otimes \mathbf{A})\boldsymbol{\Gamma}\boldsymbol{\rho} + \boldsymbol{\Sigma}\boldsymbol{\sigma} \\ &= \underbrace{\begin{bmatrix}(\mathbf{A}^H \otimes \mathbf{A})\boldsymbol{\Gamma} & \boldsymbol{\Sigma}\end{bmatrix}}_{\boldsymbol{\Phi}} \underbrace{\begin{bmatrix}\boldsymbol{\rho} \\ \boldsymbol{\sigma}\end{bmatrix}}_{\boldsymbol{\eta}}.\end{aligned} \tag{25}$$

Hence, with obvious notation, we have

$$\mathbf{r}(\boldsymbol{\theta},\boldsymbol{\eta}) \triangleq \mathbf{r}(\boldsymbol{\theta},\boldsymbol{\rho},\boldsymbol{\sigma}) = \boldsymbol{\Phi}\boldsymbol{\eta}. \tag{26}$$

3.2 COMET Estimator

Now we are ready to apply the covariance matching estimation techniques (COMET). First of all, let

$$\hat{\mathbf{r}} \triangleq \mathrm{vec}(\hat{\mathbf{R}}) \tag{27}$$

where $\hat{\mathbf{R}}$ is the sample covariance matrix of the received signal vector $\mathbf{x}[n]$

$$\hat{\mathbf{R}} = \frac{1}{N}\sum_{n=0}^{N-1} \mathbf{x}[n]\mathbf{x}^H[n]. \tag{28}$$

The COMET algorithm may be formulated as the weighted least-squares problem, whereby the estimates of $\boldsymbol{\theta}$ and $\boldsymbol{\eta}$ can be determined as [9]

$$\hat{\boldsymbol{\theta}}, \hat{\boldsymbol{\eta}} = \arg \min_{\boldsymbol{\theta}\in\mathfrak{D}_{\boldsymbol{\theta}}, \boldsymbol{\eta}\in\mathfrak{D}_{\boldsymbol{\eta}}} (\hat{\mathbf{r}} - \mathbf{r}(\boldsymbol{\theta},\boldsymbol{\eta}))^H \mathbf{W}^{-1} (\hat{\mathbf{r}} - \mathbf{r}(\boldsymbol{\theta},\boldsymbol{\eta})) \tag{29}$$

where $\mathfrak{D}_{\boldsymbol{\theta}}$ and $\mathfrak{D}_{\boldsymbol{\eta}}$ denote the admissible set of parameters $\boldsymbol{\theta}$ and $\boldsymbol{\eta}$, respectively, and the weight matrix $\mathbf{W}$ is given by

$$\mathbf{W} = \mathbb{E}\left\{(\hat{\mathbf{r}} - \mathbf{r}(\boldsymbol{\theta},\boldsymbol{\eta}))^H (\hat{\mathbf{r}} - \mathbf{r}(\boldsymbol{\theta},\boldsymbol{\eta}))\right\} = \frac{1}{N}\left(\mathbf{R}^T \otimes \mathbf{R}\right).$$

Since $\hat{\mathbf{R}}$ is a consistent estimate of $\mathbf{R}$, a large-sample ML estimate of $\boldsymbol{\theta}$ and $\boldsymbol{\eta}$ can be obtained as (29) with the replacement of $\mathbf{W}$ by $\hat{\mathbf{W}} = \hat{\mathbf{R}}^T \otimes \hat{\mathbf{R}}$, or equivalently,

$$\hat{\boldsymbol{\theta}}, \hat{\boldsymbol{\eta}} = \arg \min_{\boldsymbol{\theta}\in\mathfrak{D}_{\boldsymbol{\theta}}, \boldsymbol{\eta}\in\mathfrak{D}_{\boldsymbol{\eta}}} \left\{ J \triangleq \left\| \hat{\mathbf{W}}^{-\frac{1}{2}} (\hat{\mathbf{r}} - \boldsymbol{\Phi}\boldsymbol{\eta}) \right\|^2 \right\} \tag{30}$$

Minimization of J with respect to $\boldsymbol{\eta}$ yields

$$\hat{\boldsymbol{\eta}} = \left(\boldsymbol{\Phi}^H \hat{\mathbf{W}}^{-1} \boldsymbol{\Phi}\right)^{-1} \boldsymbol{\Phi}^H \hat{\mathbf{W}}^{-1} \hat{\mathbf{r}}. \tag{31}$$

Hence, the estimate of $\boldsymbol{\theta}$ can be obtained by inserting (31) into (30)

$$\hat{\boldsymbol{\theta}} = \arg \min_{\boldsymbol{\theta}\in\mathfrak{D}_{\boldsymbol{\theta}}} \hat{\mathbf{r}}^H \hat{\mathbf{W}}^{-\frac{1}{2}} \boldsymbol{\Pi}^{\perp}_{\hat{\mathbf{W}}^{-\frac{1}{2}}\boldsymbol{\Phi}} \hat{\mathbf{W}}^{-\frac{1}{2}} \hat{\mathbf{r}} \tag{32}$$

where

$$\begin{aligned}\boldsymbol{\Pi}_{\hat{\mathbf{W}}^{-\frac{1}{2}}\boldsymbol{\Phi}} &\triangleq \hat{\mathbf{W}}^{-\frac{1}{2}} \boldsymbol{\Phi} (\boldsymbol{\Phi}^H \hat{\mathbf{W}}^{-1} \boldsymbol{\Phi})^{-1} \boldsymbol{\Phi}^H \hat{\mathbf{W}}^{-\frac{1}{2}} \\ \boldsymbol{\Pi}^{\perp}_{\hat{\mathbf{W}}^{-\frac{1}{2}}\boldsymbol{\Phi}} &\triangleq \mathbf{I} - \boldsymbol{\Pi}_{\hat{\mathbf{W}}^{-\frac{1}{2}}\boldsymbol{\Phi}}\end{aligned} \tag{33}$$

are the orthogonal projection and orthogonal complement projection matrices of $\hat{\mathbf{W}}^{-\frac{1}{2}}\boldsymbol{\Phi}$, respectively. By using the identity (21), it can be shown that [9] $\hat{\mathbf{W}}^{-\frac{1}{2}}\hat{\mathbf{r}} = \mathrm{vec}(\mathbf{I})$ and $\hat{\mathbf{W}}^{-\frac{1}{2}}\mathrm{vec}(\mathbf{I}) = \mathrm{vec}(\hat{\mathbf{R}}^{-1})$. Therefore, the estimate of $\boldsymbol{\theta}$ can be determined by

$$\begin{aligned}\hat{\boldsymbol{\theta}} &= \arg \max_{\boldsymbol{\theta}\in\mathfrak{D}_{\boldsymbol{\theta}}} \mathrm{vec}(\mathbf{I})^H \boldsymbol{\Pi}_{\hat{\mathbf{W}}^{-\frac{1}{2}}\boldsymbol{\Phi}} \mathrm{vec}(\mathbf{I}) \\ &= \arg \max_{\boldsymbol{\theta}\in\mathfrak{D}_{\boldsymbol{\theta}}} \mathrm{vec}\left(\hat{\mathbf{R}}^{-1}\right)^H \boldsymbol{\Phi} \\ &\qquad \left(\boldsymbol{\Phi}^H \hat{\mathbf{W}}^{-1} \boldsymbol{\Phi}\right)^{-1} \boldsymbol{\Phi}^H \mathrm{vec}\left(\hat{\mathbf{R}}^{-1}\right).\end{aligned} \tag{34}$$

Once $\hat{\boldsymbol{\theta}}$ is obtained as (34), the large-sample ML estimate $\hat{\boldsymbol{\eta}}$ can be obtained as (31), and hence the fading statistics estimate $\hat{\boldsymbol{\rho}}$ and the noise parameter estimate $\hat{\boldsymbol{\sigma}}$ (cf. (25)).

3.3 Estimate Calculation

The Newton-type method is applied in [9] to perform the minimization in (34) without explicit consideration of the bound constraint (i.e., $\boldsymbol{\theta} \in \mathfrak{D}_{\boldsymbol{\theta}}$, where $\mathfrak{D}_{\boldsymbol{\theta}}$ may be determined by certain applications *a priori*) [2].

We consider here apply the pattern search methods [11] to solve this bound constrained minimization problem. The pattern search methods [11–13] are gradient-related, descent methods. In the unconstrained case, the pattern search methods work much like line-search quasi-Newton methods. The pattern search algorithms include sufficient search directions to guarantee that if the current iterate is not a stationary point, then at least one of the search directions is a descent direction. We apply the bound constrained pattern search algorithm to solve (34) to improve the search procedure. Please refer to [11–13] (and references therein) for more information on the pattern search methods.

4. SIMULATION RESULTS

In this section, the performance of the proposed method is evaluated by numerical simulations. In all the experiments, a

[2] Albeit this is not actually a serious problem with good initialization and the Newton-type algorithm is applied locally, as in [9].

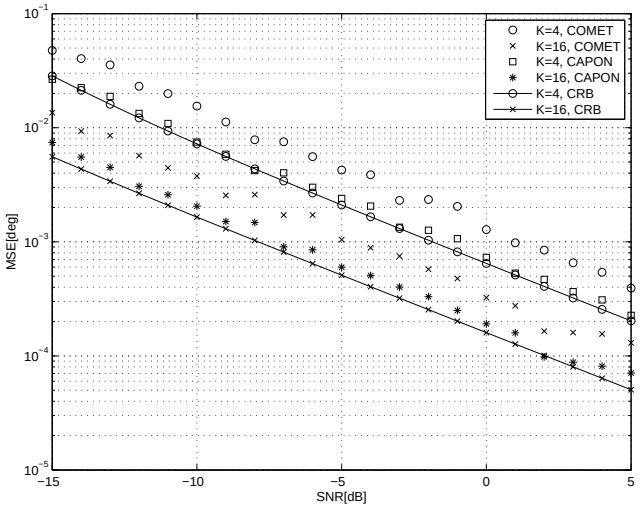

Figure 1: Angle MSE of the target located at θ_1. The number of available snapshots is 100.

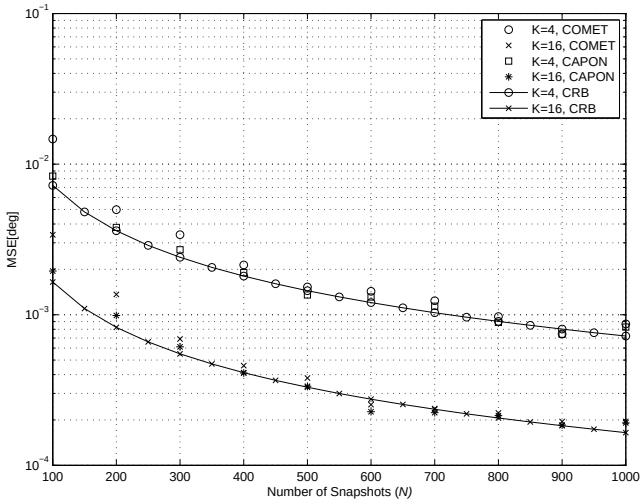

Figure 2: Angle MSE of the target located at θ_1. SNR $= -10\,$dB.

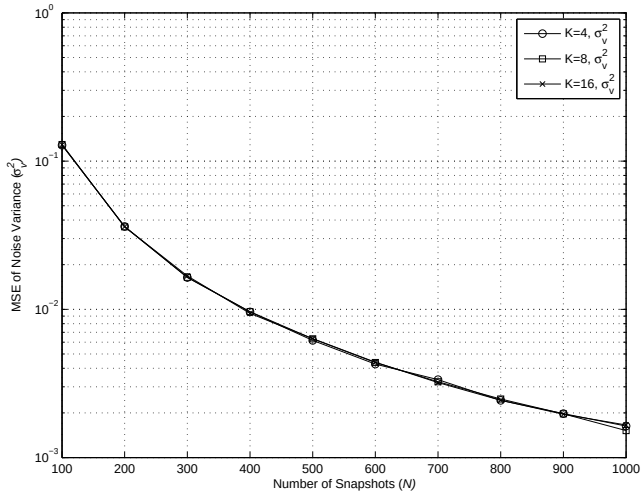

Figure 3: MSE of noise variance estimates. SNR $= -10\,$dB.

ULA of $M = 20$ antennas spaced half a wavelength apart is employed at the receiver. Two targets are located at $\theta_1 = 7^\circ$ and $\theta_2 = 15^\circ$, respectively. The additive noise is assumed to be spatially and temporally white, and the covariance matrix of the noise is given by $\mathbf{Q} = \mathbb{E}\{\mathbf{v}[n]\mathbf{v}^H[n]\} = \sigma_v^2\mathbf{I}_M$, where σ_v^2 is the average power of noise. Hence, $\mathrm{vec}(\mathbf{Q}) = \mathrm{vec}(\mathbf{I}_M)\sigma_v^2$. The signal-to-noise ratio (SNR) refers to a single snapshots. Since the transmit power of each transmit antenna is $\frac{\sigma_s^2}{K}$, the SNR at the receiver is $\frac{\mathbb{E}\{\sigma_s^2 K^{-1}\|\alpha\|^2\}}{\sigma_v^2} = \frac{\sigma_s^2}{\sigma_v^2}$ [5].

The simulated results are compared with the stochastic Cramér-Rao bound (CRB) given by [14]

$$\mathrm{CRB}(\boldsymbol{\theta}) = \frac{\sigma_v^2}{2N}\left\{\Re\left(\mathbf{D}^H\boldsymbol{\Pi}_{\mathbf{A}}^{\perp}\mathbf{D}\right)\odot\left(\mathbf{P}\mathbf{A}^H\mathbf{R}^{-1}\mathbf{A}\mathbf{P}\right)^T\right\}^{-1} \tag{35}$$

where $\Re\{\cdot\}$ and $\odot$ denote the real part of a complex value and the Hadamard-Schur product, respectively. The lth column of the $M \times L$ matrix $\mathbf{D}$ is defined to be $\mathbf{d}_l \triangleq \frac{d\boldsymbol{a}(\theta_l)}{d\theta_l}$. The matrix $\boldsymbol{\Pi}_{\mathbf{A}}^{\perp} \triangleq \mathbf{I} - \mathbf{A}\left(\mathbf{A}^H\mathbf{A}\right)^{-1}\mathbf{A}^H$ is the orthogonal complement projection matrix of $\mathbf{A}$.

The empirical mean-squared error (MSE) of the angle estimate $\hat{\theta}_l$ is defined as

$$\mathrm{MSE}(\hat{\theta}_l) \triangleq \frac{1}{T}\sum_{t=1}^{T}\left|\hat{\theta}_l^{(t)} - \theta_l\right|^2, \qquad l = 1,\cdots,L \tag{36}$$

where $\hat{\theta}_l^{(t)}$ is the angle estimate of the lth target in the tth Monte Carlo trial. The MSE of other parameter estimates may be similarly defined. In each simulation, $T = 300$ Monte Carlo trials are conducted. The Genetic Algorithm and Direct Search Toolbox for MATLAB® is used to implement the COMET algorithm.

The empirical angle MSEs of the target located at $\theta_1 = 7^\circ$ with different SNRs are shown in Fig.1. The number of available snapshots is 100. The results shown in Fig.1 indicate that the performance of the COMET algorithm improves steadily as the SNR increases. Moreover, the accuracy of the algorithm improves as the number of transmitter antennas increases. This may be interpreted as follows. The more transmit antennas are used, more pronounced spatial diversity gain can be obtained by the MIMO radar configuration, and hence the estimation accuracy improves. The stochastic CRB and the performance of Capon beamformer are also plotted for comparison.

The empirical angle MSEs of the target located at $\theta_1 = 7^\circ$ with different available snapshots are shown in Fig.2. The SNR is $-10\,$dB. Note that while the Capon estimator slightly outperforms the COMET estimator in small sample size scenarios, both estimators approach the stochastic CRB with similar performance as the sample size increases. This is no surprise since the COMET algorithm is a large-sample ML estimator.

The noise average power parameter estimation results are shown in Fig.3 as well. The noise parameter estimate is extracted from the estimate $\hat{\boldsymbol{\eta}}$ (cf. (31) and (25)). The performance improves as the number of snapshots increases since the accuracy of covariance matrix estimate improves. It can

be observed that the improvement of the noise average power estimate due to the increase of the transmit antennas seems to be not pronounced. The performance of the estimate $\hat{\boldsymbol{\rho}}$ is also demonstrated by the simulation results to improve as the number of snapshots increases, which are not plotted here.

5. CONCLUSIONS

We have considered the multiple target localization and estimation problem of a statistical MIMO radar system. We have analyzed the covariance structure of the received signals and applied the covariance matching technique to the active direction finding and parameter estimation problem. The simulation results show that the angle estimation performance improves as the transmit antennas increases. The performance of other parameter estimates is also validated through numerical simulations.

REFERENCES

[1] Eran Fishler, Alex Haimovich, Rick Blum, Dmitry Chizhik, Len Cimini, and Reinaldo Valeneuela, "MIMO radar: an idea whose time has come," in *Proc. IEEE Radar Conference*, Philadelphia, Pennsylvania, USA, Apr. 2004, pp. 71–78.

[2] Eran Fishler, Alexander Haimovich, Rick S. Blum, Jr. Leonard J. Cimini, Dmitry Chizhik, and Reinaldo A. Valenzuela, "Spatial diversity in radars—models and detection performance," *IEEE Trans. Signal Processing*, vol. 54, no. 3, pp. 823–838, Mar. 2006.

[3] Joseph Tabrikian and Ilya Bekkerman, "Transmission diversity smoothing for multi-target localization," in *Proc. IEEE International Conference on Acoustics, Speech, and Signal Processing (ICASSP '05)*, Philadelphia, Pennsylvania, USA, Mar. 2005, vol. 4, pp. 1041–1044.

[4] Luzhou Xu, Jian Li, and Petre Stoica, "Adaptive techniques for MIMO radar," in *4th IEEE Workshop Sensor Array Multi-Channel Processing*, Waltham, MA, USA, July 2006, pp. 258–262.

[5] Nikolaus H. Lehmann, Eran Fishler, Alexander M. Haimovich, Rick S. Blum, Dmitry Chizhik, Jr. Leonard J. Cimini, and Reinaldo A. Valenzuela, "Evaluation of transmit diversity in MIMO-radar direction finding," *IEEE Trans. Signal Processing*, vol. 55, no. 5, pp. 2215–2225, May 2007.

[6] Luzhou Xu and Jian Li, "Iterative generalized-likelihood ratio test for MIMO radar," *IEEE Trans. Signal Processing*, vol. 55, no. 6, pp. 2375–2385, June 2007.

[7] Ilya Bekkerman and Joseph Tabrikian, "Target detection and localization using mimo radars and sonars," *IEEE Trans. Signal Processing*, vol. 54, no. 10, pp. 3873–3883, Oct. 2006.

[8] Jian Li, Petre Stoica, and Yao Xie, "On probing signal design for MIMO radar," in *40th Asilomar Conf. Signals Systems, Computers*, Pacific Grove, CA, USA, Oct. 2006, pp. 31–35.

[9] Björn Ottersten, Petre Stoica, and Richard Roy, "Covariance matching estimation techniques for array signal processing applications," *Digital Signal processing*, vol. 8, no. 3, pp. 185–210, 1998.

[10] Wei Xia, Zishu He, and Yuyu Liao, "Subspace-based method for multiple-target localization using MIMO radars," in *Signal Processing and Information Technology, 2007 IEEE International Symposium on (ISSPIT 2007)*, Cairo, Egypt, Dec. 2007, pp. 715–720.

[11] Robert Michael Lewis and Virginia Torczon, "Pattern search algorithms for bound constrained minimization," *SIAM Journal on Optimization*, vol. 9, no. 4, pp. 1082–1099, 1999.

[12] Virginia Torczon, "On the convergence of pattern search algorithms," *SIAM Journal on Optimization*, vol. 7, no. 1, pp. 1–25, 1997.

[13] Charles Audet and J.E. Dennis Jr., "Analysis of generalized pattern searches," *SIAM Journal on Optimization*, vol. 13, no. 3, pp. 889–903, 2003.

[14] Petre Stoica, Erik G. Larsson, and Alex B. Gershman, "The stochastic CRB for array processing: a textbook derivation," *IEEE Signal Processing Lett.*, vol. 8, no. 5, pp. 148–150, May 2001.